

Stability of vertical films of molten glass due to evaporation

Franck Pigeonneau, Helena Kočárková, Florence Rouyer

► **To cite this version:**

Franck Pigeonneau, Helena Kočárková, Florence Rouyer. Stability of vertical films of molten glass due to evaporation. International Conference on Multiphase Flow, May 2013, Jeju, South Korea. 2013. <hal-01519293>

HAL Id: hal-01519293

<https://hal-mines-paristech.archives-ouvertes.fr/hal-01519293>

Submitted on 6 May 2017

HAL is a multi-disciplinary open access archive for the deposit and dissemination of scientific research documents, whether they are published or not. The documents may come from teaching and research institutions in France or abroad, or from public or private research centers.

L'archive ouverte pluridisciplinaire **HAL**, est destinée au dépôt et à la diffusion de documents scientifiques de niveau recherche, publiés ou non, émanant des établissements d'enseignement et de recherche français ou étrangers, des laboratoires publics ou privés.

Stability of vertical films of molten glass due to evaporation

F. Pigeonneau*, H. Kočárková*, F. Rouyer†

* Surface du Verre et Interfaces, UMR 125 CNRS/Saint-Gobain, Aubervilliers, France

† Laboratoire Navier, UMR CNRS 8205, Université Paris-Est Marne la Vallée, France,

Keywords: film drainage, Trouton model, molten glass, high viscous fluid, evaporation

Abstract

This work presents a theoretical model to study the gravitational drainage of a vertical molten glass film. Surface tension gradient due to the evaporation of sodium oxide from the interfaces is taken into account using a simple model with a surface tension function of the liquid film thickness. A lubrication model is derived taking into account the gradient of surface tension. The final system of equations describing the mass and the momentum conservations is numerically solved by an implicit time solver using a finite difference method at a second order in time and space. The numerical method is compared with a previous results obtained without surface tension gradient. Afterward, the numerical procedure is applied to study a film drainage of molten silica-soda-lime glass. The effect of the surface tension gradient is investigated: it is pointed that with an increase of 0.5 % of the surface tension over the spread of the film which is order of few centimeters, the liquid film reaches an equilibrium thickness in agreement with previous experimental work.

1. Introduction

Foam consists of bubbles entrapped in a liquid solution occurring in daily life of everybody as well as in many industrial processes. In most of cases, the stability of foam is a required property. Today, many investigations are devoted to the creation of stable foams. Nevertheless, in glass melting process in particular, foam can be a nuisance. Most of glass furnaces are heated by a combustion chamber above the glass bath. Consequently, if a large part of the bath surface is recovered of foam, heat transfer, mainly radiative¹, decreases due to the insulator property of glass foam.

Glass melting is a chemical process for which glass is made in most of cases with silica, soda ash, and lime. The raw materials are generally carbonaceous elements giving a carbon dioxide release. The low solubility of CO₂ leads to a creation of large quantity of bubbles entrapped in the molten glass. To remove these gaseous inclusions, sulfate compounds are added to raw materials. Gases liberated by sulfate decomposition lead to a raising of bubble size. Due to buoyancy forces, bubbles can escape from bath surface, see Shelby (1997).

The onset of foaming has been studied by Kim and Hrma (1992), who, from a knowledge of chemical reac-

tions produced by sulfate species, determined the foaming temperature. Pilon (2002) developed a model to study the foam formation by bubbling and established a relationship between foam layer and physical properties of liquid using a dimensional analysis. Kappel et al. (1987) achieved an experimental study about film drainage on molten glass. They found that the film thickness decreases exponentially with time. They observed a stabilization state for which the film thickness was around one hundred nanometers. Laimböck (1998) did a similar experiments using the electric resistivity of molten glass to determine the film thickness. He found that glass film can reach a stabilized thickness in the same order of magnitude found by Kappel et al. (1987). Laimböck proposed a model to explain the film stability based only on the static equilibrium. The purpose of this work is to carefully study the drainage of a vertical film.

The mathematical model to describe the two-dimensional draining film has been studied by different authors as for instance Schwartz and Roy (1999). The behaviors of mobile and immobile soap films were investigated. Howell (1996) presented a general method to obtain lubrication model of thin film model in various situations. A work has been done by Braun et al. (1999, 2002) and Naire et al. (2000) for which the drainage of vertical film has been studied taking into account the Marangoni stress and the transport of surfactant agent. The role playing by thermal gradient on the surface ten-

¹The typical value of temperature is the combustion chamber is greater than 2000 K.

sion has been recently studied by Scheid et al. (2010), they shown that it is possible to form a stable liquid film controlled by the thermal gradient. In this work, the purpose is to present a lubrication model taking into account the surface tension gradient according the prior development of Howell (1996).

The second section is devoted to a model giving the behavior of the surface tension as a function of the film thickness according the recent work of Pigeonneau et al. (2012). The lubrication model is presented in section 3. The numerical development is given in §4. Results and discussion are developed in section 5 before to conclude.

2. Surface tension in molten glass and variation with the film thickness

Laimböck (1998) achieved an experimental work on a drainage of molten glass film achieved by dropping and dipping a Platinum loop in a crucible. He observed that after a fast drainage, the film thickness decreases very slowly. He proposed an explanation of this phenomena based on the change of the surface tension as a function of the film thickness. Using XPS measurement, Laimböck (1998) observed that the glass composition through the film thickness changes significantly: the Na₂O content increases strongly at the liquid/air interface while the SiO₂ content decreases. He proposed a simple model to describe the Na₂O content in the film using a mass balance assuming Na₂O adsorption.

More recently, Pigeonneau et al. (2012) achieved the same kind of experiments but observed a decrease of sodium oxide close to the interfaces. Recall that Na₂O is known to be a volatile species (Sanders and Haller 1977; Beerkens 2001). The evaporation of Na₂O leads to a modification of the glass composition at the interface. The evaporation of Na₂O is generally explained by a heterogeneous chemical reaction between water vapor and sodium oxide giving sodium hydroxide, NaOH. Consequently, it is expected to observe a positive gradient of Na over the depth of the film meaning a volatilization as it is measured in our chemical analysis (Pigeonneau et al. 2012).

The full problem involves transient diffusion process with a mass transfer coefficient between the film and the atmosphere difficult to evaluate. So, the aim of this section is to provide a simple model to describe the variation of the surface tension as a function of film thickness.

According to an additivity principle, Scholze (1990) writes the surface tension of glass as follows:

$$\gamma = \sum_{i=1}^N \gamma_i y_i, \quad (1)$$

where γ is the surface tension, N is the number of oxides

in the glass composition, y_i the mass fraction of the oxide i and γ_i is a factor corresponding to the contribution of the oxide i in the surface tension given in N/m.

Since the surface tension is determined from the bulk quantities and that Na₂O evaporate, we consider the volatilization of Na₂O to describe the change of surface tension. When the film is pulled out, the volatilization occurs leading to a decrease of Na₂O concentration. To determine this quantity for a portion of film of volume V and constant thickness h , the mass balance before and after the evaporation is given by

$$\rho_{\text{Na}_2\text{O},0}V = \rho_{\text{Na}_2\text{O}}V + 2\frac{dm_{\text{Na}_2\text{O}}}{dS}S, \quad (2)$$

in which $\rho_{\text{Na}_2\text{O},0}$ is the mass concentration of Na₂O in the bulk and $\rho_{\text{Na}_2\text{O}}$ the mass concentration in the liquid film, V the volume of the film and S the area of each interface. Finally, $dm_{\text{Na}_2\text{O}}/dS$ is the mass loss by unit surface. Since the ratio of S over V is directly the film thickness, h , the last equation can be written as follows

$$\rho_{\text{Na}_2\text{O},0}h = \rho_{\text{Na}_2\text{O}}h + 2\frac{dm_{\text{Na}_2\text{O}}}{dS}. \quad (3)$$

This equation is similar in appearance to the one used to describe the soap films just after the pulling out but with different physics (de Gennes 2001). To close this equation, we assume that the loss of mass is proportional to $\rho_{\text{Na}_2\text{O}}$ inside the portion of film of thickness h and to the size δ over which the volatilization occurs as proposed in (Pigeonneau et al. 2012):

$$\frac{dm_{\text{Na}_2\text{O}}}{dS} = \delta\rho_{\text{Na}_2\text{O}}. \quad (4)$$

This assumption is similar to the Langmuir isotherm used by Ruckenstein and Jain (1974) to study the rupture of thin liquid film with a soluble surface active agents. Remark that Laimböck (1998) took the same approximation assuming the sodium oxide is adsorbed whereas we argue that the sodium oxide is evaporated. By combining Eqs. (3) and (4), the mass concentration of Na₂O in a portion of film of thickness h is given by

$$\rho_{\text{Na}_2\text{O}} = \frac{\rho_{\text{Na}_2\text{O},0}}{1 + 2\delta/h}. \quad (5)$$

So, this phenomenological relationship leads to a closed equation to describe the mass concentration of Na₂O as a function of the film thickness. Finally, the difference of mass concentration of Na₂O in a film of thickness h and the bulk that will be used to describe the change of surface tension, is given by

$$\rho_{\text{Na}_2\text{O}} - \rho_{\text{Na}_2\text{O},0} = -\frac{\rho_{\text{Na}_2\text{O},0}}{1 + h/(2\delta)}. \quad (6)$$

This last equation can be used to evaluate the feature of surface tension as a function of film thickness. Indeed, if we assume that the surface tension changes only due to the mass concentration of Na_2O , SiO_2 and CaO which are the main oxides in the glass, the difference between the surface tension for a very thin film, γ , and a surface tension of bulk glass, γ_0 , is given according to (1) by

$$\gamma - \gamma_0 = \gamma_{\text{Na}_2\text{O}}(y_{\text{Na}_2\text{O}} - y_{\text{Na}_2\text{O},0}) + \gamma_{\text{SiO}_2}(y_{\text{SiO}_2} - y_{\text{SiO}_2,0}) + \gamma_{\text{CaO}}(y_{\text{CaO}} - y_{\text{CaO},0}). \quad (7)$$

By assuming that the decrease of the concentration of Na_2O is compensated by the increase of SiO_2 and CaO proportionally to their mutual initial weight ratio, the surface tension becomes

$$\gamma = \gamma_0 + \delta\gamma f_\gamma(h/2), \quad (8)$$

where $\delta\gamma$ is given by

$$\delta\gamma = \left(\gamma_{\text{SiO}_2} \frac{y_{\text{SiO}_2,0}}{y_{\text{SiO}_2,0} + y_{\text{CaO},0}} + \gamma_{\text{CaO}} \frac{y_{\text{CaO},0}}{y_{\text{SiO}_2,0} + y_{\text{CaO},0}} - \gamma_{\text{Na}_2\text{O}} \right) y_{\text{Na}_2\text{O},0}, \quad (9)$$

and $f_\gamma(\chi)$, where $\chi \in [-h/2; h/2]$, is an even function given by

$$f_\gamma(\chi) = \frac{1}{1 + |\chi|/\delta}. \quad (10)$$

From the factors γ_{SiO_2} , γ_{CaO} and $\gamma_{\text{Na}_2\text{O}}$ provided in Scholze (1990) and Rubenstein (1964) and with the glass composition composed by 70 wt % of SiO_2 , 15 wt % of Na_2O and 15 wt % of CaO , $\delta\gamma$ is a positive quantity meaning that the surface tension given by (8) increases when the film thickness decreases. While the scale, δ , over which the sodium oxide evaporates depends on temperature (Pigeonneau et al. 2012), the quantity $\delta\gamma$ is only a function of the glass nature. Its value is equal to $4.2 \cdot 10^{-2}$ N/m whilst the surface tension γ_0 is equal to $3.2 \cdot 10^{-1}$ N/m for the largest temperature $T = 1400^\circ\text{C}$. According to this modeling, the relative increase of surface tension is at the maximum equal to 1.5% for $h \rightarrow 0$ and of the order of 0.5% for $h \simeq 5\delta$. This last value seems appropriate for quantifying the Marangoni stress due to evaporation for thin film whose thickness $h \sim 100$ nm and whose Na_2O variation is observed over a depth equal to 20 nm (Pigeonneau et al. 2012).

3. Lubrication model of 2D-Cartesian film

This section is devoted to the derivation of the lubrication film equations in the Cartesian framework. The situation addressed in this work is shown in Fig. 1. A

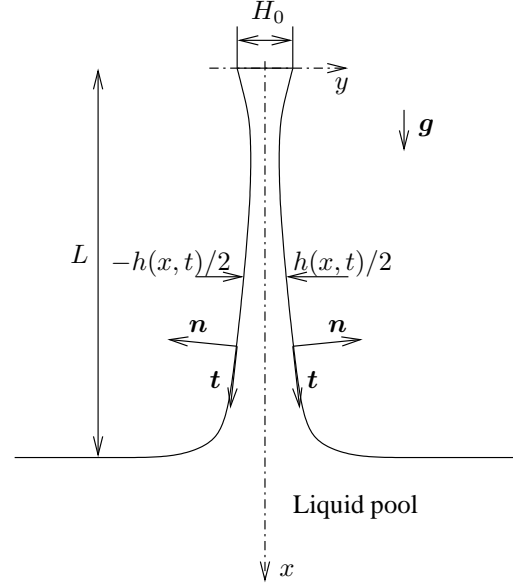


Figure 1: Liquid film draining under the gravity force. Figure is not on scale.

vertical film is attached to a wire in $x = 0$ where x represents the longitudinal direction of the film while y is the transversal coordinate. Under the gravity force directed along x , the film thickness, h , changes with the time t and depends also on x . The film has a height equal to L and falls in a liquid pool. In the following, the film thickness H_0 on $x = 0$ is assumed to be very small compare to the height L . Moreover, the film stays symmetric following the y coordinate.

Note that in a first reading, this section can be dropped and the reader can directly go to the beginning of section 4 where the lubrication model is summed-up.

3.1. Problem statement

The purpose of this section is to determine the equations of the motion using the lubrication theory. In order to do that we start from the general equations of the fluid dynamics written in the Cartesian reference frame. The liquid is assumed incompressible and the dynamic viscosity is taken constant. The continuity and momentum equations are written as follows:

$$u_{,x} + v_{,y} = 0, \quad (11)$$

$$u_{,t} + uu_{,x} + vv_{,y} = -\frac{P_{,x}}{\rho} + \nu(u_{,xx} + u_{,yy}) + g, \quad (12)$$

$$v_{,t} + uv_{,x} + vv_{,y} = -\frac{P_{,y}}{\rho} + \nu(v_{,xx} + v_{,yy}), \quad (13)$$

where u and v are the velocity components over x and y respectively and P the pressure. The quantity, ν , is the kinematic viscosity defined by μ/ρ where ρ is the

density. In the last equations, the Jacobian notation is used to represent the partial derivative over x and y where $u_{,x}$ is equal to $\partial u/\partial x$ for instance.

These equations must be completed by boundary conditions. On $x = 0$, the no-slip condition is used:

$$u(0, y, t) = v(0, y, t) = 0. \quad (14)$$

On the free surface representing the frontiers of the film, two kinds of boundary conditions are used: the first is a kinematic condition given by

$$v(x, \pm h/2, t) = \pm \frac{1}{2} \left[\frac{\partial h}{\partial t} + u(x, \pm h/2, t) \frac{\partial h}{\partial x} \right] \quad (15)$$

written in $\pm h/2$ where the upper sign is used in $y = h/2$ and the lower sign in $y = -h/2$.

The second condition is obtained from the momentum balance written at the interface between two fluids. This last one is decomposed in two following relationships:

$$\mathbf{n} \cdot \boldsymbol{\sigma} \cdot \mathbf{n} = -\gamma \kappa, \quad (16)$$

$$\mathbf{t} \cdot \boldsymbol{\sigma} \cdot \mathbf{n} = \mathbf{grad} \gamma \cdot \mathbf{t}, \quad (17)$$

where γ is the surface tension, \mathbf{n} the unit normal vector to the interface, \mathbf{t} the unit tangential vector and κ is the average curvature. Following the development given in §2, the surface tension is a function of h meaning that the partial derivative over y is equal to zero. The quantities \mathbf{n} , \mathbf{t} and κ are given by

$$\mathbf{n} = \frac{1}{\sqrt{1 + h_{,x}^2/4}} \left(-\frac{h_{,x}}{2} \mathbf{e}_x \pm \mathbf{e}_y \right), \quad (18)$$

$$\mathbf{t} = \frac{1}{\sqrt{1 + h_{,x}^2/4}} \left(\mathbf{e}_x \pm \frac{h_{,x}}{2} \mathbf{e}_y \right), \quad (19)$$

$$\kappa = -\frac{h_{,xx}}{2(1 + h_{,x}^2/4)^{3/2}}. \quad (20)$$

From these definitions of geometrical quantities, Eqs. (16) and (17) become

$$-P + \frac{2\mu}{1 + h_{,x}^2/4} \left[\frac{h_{,x}^2}{4} u_{,x} + v_{,y} \mp \frac{h_{,x}}{2} (u_{,y} + v_{,x}) \right] = \frac{\gamma h_{,xx}}{2(1 + h_{,x}^2/4)^{3/2}}, \quad (21)$$

$$\mu h_{,x} (v_{,y} - u_{,x}) \pm \mu \left(1 - \frac{h_{,x}^2}{4} \right) (u_{,y} + v_{,x}) = \gamma_{,x} \sqrt{1 + h_{,x}^2/4}, \quad (22)$$

in $y = \pm h(x, t)/2$.

Close to the liquid pool, the film behaves as a static meniscus: the force balance is achieved between the surface tension and gravity forces. This equilibrium can be written as follows, (Naire et al. 2000)

$$\kappa_{,x} = \frac{1}{l_c^2}, \quad (23)$$

where l_c is the capillary length defined by

$$l_c = \sqrt{\frac{\gamma}{\rho g}}. \quad (24)$$

Eq. (23) will be used in the following to specify the boundary conditions in $x = L$.

The system of equations written above is used to establish the lubrication equations. In order to do that, the problem must be normalized which is done in the next subsection.

3.2. Scaling and dimensionless equations

Since the length of the liquid film is L , the longitudinal coordinate is normalized as follows

$$\bar{x} = \frac{x}{L}. \quad (25)$$

For the y coordinate, the typical scale is given by H_0 so we put

$$\bar{y} = \frac{y}{H_0}. \quad (26)$$

The film thickness is written as follows

$$\bar{h} = \frac{h}{H_0}. \quad (27)$$

The ratio $\epsilon = \frac{H_0}{L}$ is assumed smaller than one. From this statement, the two dimensionless velocity components are written as follows

$$\bar{u} = \frac{u}{U_0}, \quad (28)$$

$$\bar{v} = \frac{v}{\epsilon U_0}, \quad (29)$$

where U_0 is a characteristic velocity determined from the equilibrium of longitudinal viscous stress and the gravity force given by

$$U_0 = \frac{\rho g L^2}{\mu}. \quad (30)$$

The pressure and time are respectively normalized by

$$\bar{P} = \frac{P}{\mu U_0 / L}, \quad (31)$$

$$\bar{t} = \frac{t U_0}{L}. \quad (32)$$

According to (8), the surface tension is written like this

$$\gamma = \gamma_0 + \delta\gamma f_\gamma(h/2), \quad (33)$$

where $f_\gamma(\chi)$ is a dimensionless even function defined in §2, Eq. (10).

By dividing by γ_0 , the dimensionless surface tension becomes

$$\bar{\gamma} = 1 + \overline{\delta\gamma} f_\gamma(\bar{h}/2), \quad (34)$$

with

$$\overline{\delta\gamma} = \frac{\delta\gamma}{\gamma_0}. \quad (35)$$

In the following, the quantity $\overline{\delta\gamma}$ is assumed sufficiently small to take $\bar{\gamma}$ equal to one.

The nondimensional equations of motion and boundary conditions, dropping the bar over the dimensionless variables, are

$$u_{,x} + v_{,y} = 0, \quad (36)$$

$$\epsilon^2 \text{Re} (u_{,t} + uu_{,x} + vv_{,y}) = -\epsilon^2 P_{,x} + \epsilon^2 u_{,xx} + u_{,yy} + \epsilon^2, \quad (37)$$

$$\epsilon^2 \text{Re} (v_{,t} + uv_{,x} + vv_{,y}) = -P_{,y} + \epsilon^2 v_{,xx} + v_{,yy}, \quad (38)$$

in the liquid film where Re is the Reynolds number equal to

$$\text{Re} = \frac{\rho U_0 L}{\mu}. \quad (39)$$

The kinematic conditions are

$$v(x, \pm h/2, t) = \pm \frac{1}{2} \left[\frac{\partial h}{\partial t} + u(x, \pm h/2, t) \frac{\partial h}{\partial x} \right] \quad (40)$$

in $\pm h/2$ and the jump stress conditions are

$$-P + \frac{2}{1 + \epsilon^2 h_{,x}^2} \left[\frac{\epsilon^2 h_{,x}^2}{4} u_{,x} + v_{,y} \mp \frac{h_{,x}}{2} (u_{,y} + \epsilon^2 v_{,x}) \right] = \frac{1}{\text{Bo}} \frac{\gamma h_{,xx}}{2(1 + \epsilon^2 h_{,x}/4)^{3/2}}, \quad (41)$$

$$\epsilon^2 h_{,x} (v_{,y} - u_{,x}) \pm \left(1 - \epsilon^2 \frac{h_{,x}^2}{4} \right) (u_{,y} + \epsilon^2 v_{,x}) = \pm \text{Ma} \epsilon^2 \frac{df_\gamma}{d\chi} \frac{h_{,x}}{2} \sqrt{1 + \epsilon^2 h_{,x}^2/4}, \quad (42)$$

with

$$\text{Bo} = \frac{\rho g L^3}{\gamma_0 H_0}, \quad (43)$$

$$\text{Ma} = \frac{\delta\gamma}{\mu U_0}. \quad (44)$$

The quantity Bo is a Bond number and Ma a Marangoni number.

3.3. Lubrication model

From the previous developments, the equations depends on a small parameter ϵ^2 . The lubrication model consists to expand each unknown in a power of ϵ^2 as for instance

$$u(x, y, t; \epsilon^2) = u_0(x, y, t) + \epsilon^2 u_1(x, y, t) + \dots \quad (45)$$

If the equations of motion in the liquid film, Eqs. (36-38), are easy to expand as a function of ϵ^2 , the boundary conditions are more difficult to develop. This is due to that the boundary conditions are applied on $\pm h/2$ where h must be also expanded as a function of ϵ^2 . Consequently, the boundary conditions must be projected on the film thickness at zeroth order h_0 where h is expanded like

$$h(x, t; \epsilon^2) = h_0(x, t) + \epsilon^2 h_1(x, t) + \dots \quad (46)$$

In the following, we sum up the determination of the lubrication model without giving all details.

3.3.1. Equations at the zeroth order

At the zeroth order, the equations of motion are

$$u_{0,x} + v_{0,y} = 0, \quad (47)$$

$$u_{0,yy} = 0, \quad (48)$$

$$-P_{0,y} + v_{0,yy} = 0. \quad (49)$$

The boundary conditions in $\pm h_0/2$ are:

$$v_0(x, \pm h_0/2, t) = \pm \frac{1}{2} \left[\frac{\partial h_0}{\partial t} + u_0(x, \pm h_0/2, t) \frac{\partial h_0}{\partial x} \right], \quad (50)$$

$$-P_0 + 2v_{0,y} = \frac{h_{0,xx}}{2\text{Bo}}, \quad (51)$$

$$u_{0,y} = 0. \quad (52)$$

It is easy to see that u_0 depend only on x and t as well as the pressure which can be given by

$$P_0(x, t) = -2u_{0,x} - \frac{h_{0,xx}}{2\text{Bo}}. \quad (53)$$

Moreover, v_0 can be written as follows

$$v_0(x, y, t) = -yu_{0,x}. \quad (54)$$

Using the kinematic conditions, Eq. (50), the continuity equation

$$\frac{\partial h_0}{\partial t} + \frac{\partial(h_0 u_0)}{\partial x} = 0, \quad (55)$$

is established.

Nevertheless, the velocity component $u_0(x, t)$ is unknown requiring another equation obtained from the first order solution.

3.3.2. Equations at the first order

To find a supplementary equation, we use the method described in (Howell 1996) where the momentum equation over x coordinate is written. From the expansion as a function of ϵ^2 , the momentum equation along x is given by:

$$u_{1,yy} = \text{Re} (u_{0,t} + u_0 u_{0,x}) - 3u_{0,xx} - \frac{h_{0,xxx}}{2 \text{Bo}} - 1, \quad (56)$$

where the pressure P_0 given by (53) has been used. The integration of the last equation over y gives the relationship

$$u_{1,y}(x, h_0/2, t) - u_{1,y}(x, -h_0/2, t) = \text{Re} h_0 (u_{0,t} + u_0 u_{0,x}) - 3h_0 u_{0,xx} - \frac{h_0 h_{0,xxx}}{2 \text{Bo}} - h_0. \quad (57)$$

The boundary conditions at the first order show that $u_{1,y}(x, \pm h_0/2, t)$ can be written like

$$u_{1,y}(x, \pm h_0/2, t) = \pm \left[2u_{0,x} h_{0,x} + \frac{h_0}{2} u_{0,xx} + \text{Ma} \frac{df_\gamma}{d\chi} \frac{h_{0,x}}{2} \right], \quad (58)$$

which is only a function of the unknowns at the zeroth order.

Finally, the momentum equation over x coordinate is written as follows

$$\text{Re} \left[\frac{\partial(h_0 u_0)}{\partial t} + \frac{\partial(h_0 u_0 u_0)}{\partial x} \right] = 4 \frac{\partial(h_0 u_{0,x})}{\partial x} + \frac{h_0 h_{0,xxx}}{2 \text{Bo}} + \text{Ma} \frac{df_\gamma}{d\chi} h_{0,x} + h_0. \quad (59)$$

The left hand side is the inertial contribution. The first term in the right hand side is the extensional viscous force, the second is the surface tension force due to the gradient of curvature, the third term is the force due to the surface tension gradient and the last is the gravity force.

With the two equations (55) and (59), the Cauchy problem is well determined for the two unknowns h_0 and u_0 . The last point is to establish the boundary conditions on $x = 0$ and 1 and the initial condition which are presented at the beginning of the numerical part.

4. Numerical method

We address in this section the numerical method to solve the drainage equation of two-dimensional film obtained at the zeroth order. In the following the index 0 in the unknowns are removed. Note that the problem here stays

under dimensionless form. The two-coupled equations to solve are recalled here:

$$\begin{aligned} \frac{\partial h}{\partial t} + \frac{\partial(hu)}{\partial x} &= 0, \quad (60) \\ \text{Re} h \left(\frac{\partial u}{\partial t} + uu_{,x} \right) &= 4 \frac{\partial(hu_{,x})}{\partial x} + \frac{hh_{,xxx}}{2 \text{Bo}} + \\ &\text{Ma} \frac{df_\gamma}{d\chi} h_{,x} + h. \quad (61) \end{aligned}$$

The function f_γ is given by (10). At the top of the film, the boundary conditions are:

$$h(0, t) = 1, \quad (62)$$

$$u(0, t) = 0. \quad (63)$$

For the bottom, the behavior of the static meniscus is used as already pointed out by Ruschak (1978) and Naire et al. (2000). For $x = 1$, we impose the first and the second derivatives of h :

$$h_{,x}(1, t) = \alpha, \quad (64)$$

$$h_{,xx}(1, t) = \beta = \frac{2}{\epsilon l_c} \sqrt{\left(2 - \frac{\epsilon \alpha}{K}\right) K^3}, \quad (65)$$

$$\text{with } K = \sqrt{1 + \epsilon^2 \alpha^2 / 4}. \quad (66)$$

The condition on $h_{,xx}$ is obtaining from the equation of the static meniscus (see detail of derivation in Annex A). The boundary condition is stayed free for the velocity at the bottom of the film.

At the initial time, h is imposed by

$$h(x, 0) = 1, \quad (67)$$

for $x \in [0; x_c]$ and

$$h(x, 0) = 1 - (\alpha - \beta)x_c - \frac{\beta x_c^2}{2} + (\alpha - \beta)x - \frac{\beta x^2}{2}, \quad (68)$$

for $x \in]x_c; 1]$ where α and β are the coefficients used in the boundary conditions on $x = 1$ given previously and x_c is given by

$$x_c = 1 - \frac{\alpha}{\beta}. \quad (69)$$

The velocity u is assumed to be equal to zero at $t = 0$.

To solve the coupled equations, (60) and (61), a finite difference method is used. The x space is divided in N elements where a discrete values of x_i are given by

$$x_i = \frac{i}{N}, \quad (70)$$

where i varies from 0 to N . The derivatives in space and time are determined at the second order in time and space, $\mathcal{O}(\Delta t^2, \Delta x^2)$ where Δt is the time step and $\Delta x = 1/N$. According Press et al. (1992); Fletcher

(1991), a centered schemes are used for all space derivatives apart from nodes $i = 1$ and $N - 1$ where the third derivative of h must be determined with unsymmetric schemes (Collatz 1960).

Defining h_i^k and u_i^k as the film thickness and the velocity respectively at the time iteration k and in x_i , the discrete form of Eqs. (60) and (61) for $i = 2$ to $N - 2$ is given by

$$\frac{3h_i^{k+1} - 4h_i^k + h_i^{k-1}}{\Delta t} + \frac{h_{i+1}^{k+1}u_{i+1}^{k+1} - h_{i-1}^{k+1}u_{i-1}^{k+1}}{\Delta x} = 0, \quad (71)$$

$$\begin{aligned} & \text{Re } h_i^{k+1} \frac{3u_i^{k+1} - 4u_i^k + u_i^{k-1}}{\Delta t} + \text{Re } h_i^{k+1} u_i^{k+1} \\ & \frac{u_{i+1}^{k+1} - u_{i-1}^{k+1}}{\Delta x} - 4 \left[(h_i^{k+1} + h_{i-1}^{k+1}) u_{i-1}^{k+1} \right. \\ & \quad \left. - (h_{i-1}^{k+1} + 2h_i^{k+1} + h_{i+1}^{k+1}) u_i^{k+1} + \right. \\ & \quad \left. (h_i^{k+1} + h_{i+1}^{k+1}) u_{i+1}^{k+1} \right] / \Delta x^2 - \\ & \frac{h_i^{k+1}}{2 \text{Bo}} \frac{h_{i+2}^{k+1} - 2h_{i+1}^{k+1} + 2h_{i-1}^{k+1} - h_{i-2}^{k+1}}{\Delta x^3} - \\ & \text{Ma} \frac{df_\gamma(h_i^{k+1}/2)}{d\chi} \frac{h_{i+1}^{k+1} - h_{i-1}^{k+1}}{\Delta x} - 2h_i^{k+1} = 0. \quad (72) \end{aligned}$$

For $i = 1$, the momentum equation is modified by taking an upward scheme (Collatz 1960) to determine the third derivative of h as follows

$$\begin{aligned} & \text{Re } h_i^{k+1} \frac{3u_i^{k+1} - 4u_i^k + u_i^{k-1}}{\Delta t} + \text{Re } h_i^{k+1} u_i^{k+1} \\ & \frac{u_{i+1}^{k+1} - u_{i-1}^{k+1}}{\Delta x} - 4 \left[(h_i^{k+1} + h_{i-1}^{k+1}) u_{i-1}^{k+1} \right. \\ & \quad \left. - (h_{i-1}^{k+1} + 2h_i^{k+1} + h_{i+1}^{k+1}) u_i^{k+1} + \right. \\ & \quad \left. (h_i^{k+1} + h_{i+1}^{k+1}) u_{i+1}^{k+1} \right] / \Delta x^2 - \\ & \frac{h_i^{k+1}}{2 \text{Bo}} \left[-3h_{i-2}^{k+1} + 10h_i^{k+1} - 12h_{i+1}^{k+1} + \right. \\ & \left. 6h_{i+2}^{k+1} - h_{i+3}^{k+1} \right] / \Delta x^3 - \text{Ma} \frac{df_\gamma(h_i^{k+1}/2)}{d\chi} \\ & \frac{h_{i+1}^{k+1} - h_{i-1}^{k+1}}{\Delta x} - 2h_i^{k+1} = 0, \quad (73) \end{aligned}$$

and for $i = N - 1$, a downward scheme (Collatz 1960)

is used given the relationship

$$\begin{aligned} & \text{Re } h_i^{k+1} \frac{3u_i^{k+1} - 4u_i^k + u_i^{k-1}}{\Delta t} + \text{Re } h_i^{k+1} u_i^{k+1} \\ & \frac{u_{i+1}^{k+1} - u_{i-1}^{k+1}}{\Delta x} - 4 \left[(h_i^{k+1} + h_{i-1}^{k+1}) u_{i-1}^{k+1} \right. \\ & \quad \left. - (h_{i-1}^{k+1} + 2h_i^{k+1} + h_{i+1}^{k+1}) u_i^{k+1} + \right. \\ & \quad \left. (h_i^{k+1} + h_{i+1}^{k+1}) u_{i+1}^{k+1} \right] / \Delta x^2 - \\ & \frac{h_i^{k+1}}{2 \text{Bo}} \left[3h_{i+1}^{k+1} - 10h_i^{k+1} + 12h_{i+1}^{k-1} - \right. \\ & \left. 6h_{i-2}^{k+1} + h_{i-3}^{k+1} \right] / \Delta x^3 - \text{Ma} \frac{df_\gamma(h_i^{k+1}/2)}{d\chi} \\ & \frac{h_{i+1}^{k+1} - h_{i-1}^{k+1}}{\Delta x} - 2h_i^{k+1} = 0, \quad (74) \end{aligned}$$

For the boundary conditions in $i = N$ ($x = 1$), downward schemes (Collatz 1960) are used given the relationships

$$\frac{3h_N^{k+1} - 4h_{N-1}^{k+1} + h_{N-2}^{k+1}}{2\Delta x} = \alpha, \quad (75)$$

$$\frac{2h_N^{k+1} - 5h_{N-1}^{k+1} + 4h_{N-2}^{k+1} - h_{N-3}^{k+1}}{\Delta x^2} = \beta. \quad (76)$$

The system of non-linear equations is solved using a Newton scheme (D eminovith and Maron 1979).

5. Results and discussion

5.1. Test without surface tension gradient

In this first subsection, we address a computation with a Dirichlet boundary conditions applied at the top and the bottom where $h = 1$ and $u = 0$. The gradient of surface tension is not taken into account. Furthermore, the viscosity is assumed sufficiently large to neglect the inertia force in the momentum equation, (61). As consequence, the problem depends only on one parameter: the Bond number. The problem has been previously studied by Schwartz and Roy (1999). In the limit of large Bond number, the surface tension force can be removed. In this situation, Schwartz and Roy (1999) determined a self-similar solution given by

$$h(x, t) = \frac{te^{t(x-1)/4}}{4(1 - e^{-t/4})}, \quad (77)$$

$$u(x, t) = \frac{1 - e^{-tx/4}}{t(1 - e^{-t/4})} - \frac{x}{t}. \quad (78)$$

Remark that the boundary conditions on h are not fulfilled with equation (77). In fact, this solution can be

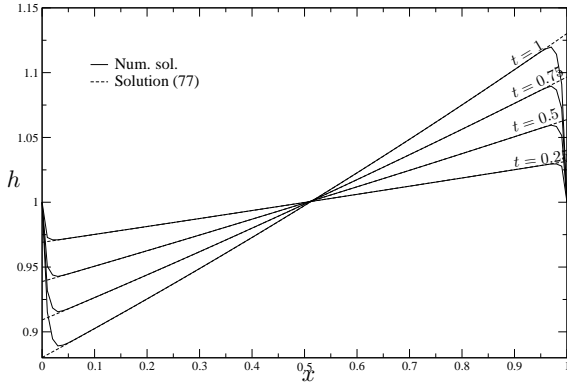


Figure 2: Film thickness, h , as a function of x with $h = 0$ and $u = 0$ at the top and the bottom and for $t = 0.25, 0.5, 0.75$ and 1 . Comparison with the self-similar solution of Schwartz and Roy (1999).

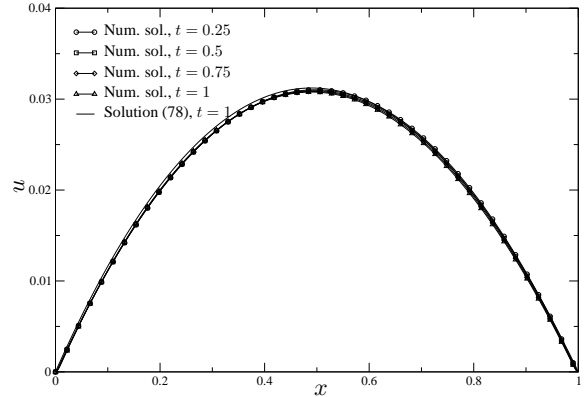


Figure 3: Film velocity, u , as a function of x with $h = 0$ and $u = 0$ at the top and the bottom and for $t = 0.25, 0.5, 0.75$ and 1 . Comparison with the self-similar solution of Schwartz and Roy (1999).

seen as an exterior solution. Indeed, close to the boundaries where the curvature changes sharply, the surface tension force can not be neglected. Furthermore, the integration over x between 0 to 1 of h given by (77) shows that the average of h stays equal to 1 whatever t .

Figure 2 shows the film thickness versus x for t equal to 0.25, 0.5, 0.75 and 1 obtaining for a Reynolds number equal to zero and a Bond number equal to 1729. Numerically, N is taken equal to 200 and $\Delta t = 10^{-2}$. The profile of the film thickness presents an anti-symmetry around the point $x = 1/2$. As mentioned above, the integration of h over x stays equal to one. This result is a consequence of the mass conservation which is very well verified numerically since the average of h when $t = 1$ is equal to 1.0024. From apart the area close to the top and the bottom of the film, the comparison between the self-solution (77) and the numerical results is good.

The velocity profiles obtained numerically are plotted in Figure 3 for $t = 0.25, 0.5, 0.75$ and 1 . The velocity profile does not change a lot with t . The solution given by (78) is computed when $t = 1$ showing the good result obtained with the numerical method.

Close to the top and the bottom, the film thickness exhibits a strong variation that can not be evidenced with the self-similar solution given by (77). Nevertheless, a simple scaling analysis gives that the order of magnitude of the boundary layer must be equal to $1/\sqrt{Bo}$. In this case, close to the boundary, the force balance is between viscous term and surface tension one. In order to control this scaling, numerical computations have been done with various Bond number in the range of [460; 60000]. Figure 4 gives the behavior of h as a function of x when $t = 1$ and for five Bond numbers. Outside of the bound-

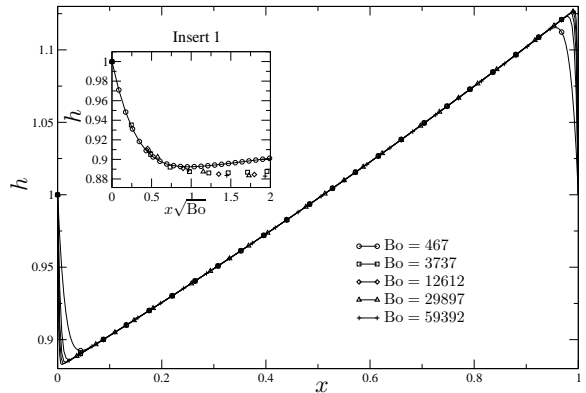


Figure 4: Film thickness, h , as a function of x with $h = 1$ and $u = 0$ at the top and the bottom and for $t = 1$ and for five Bond numbers. Insert 1 presents h as function of the stretched coordinate, $x\sqrt{Bo}$.

aries, the five profiles are quasi-identical. In order to control the scaling of the boundary layer as a function of the Bond number, h is plotted versus the stretched coordinate, $x\sqrt{Bo}$ in the insert 1 where the scaling is very well verified.

5.2. Effect of the boundary conditions at the bottom

In this subsection, the drainage of vertical film is investigated for which the coupled equations (60) and (61) are solved with the conditions given by Eqs. (62-65). The physical properties are taken from data corresponding to silica-soda-lime glass with a nominal composition of 70 wt % of SiO_2 , 15 wt % of Na_2O and 15 wt % of CaO .

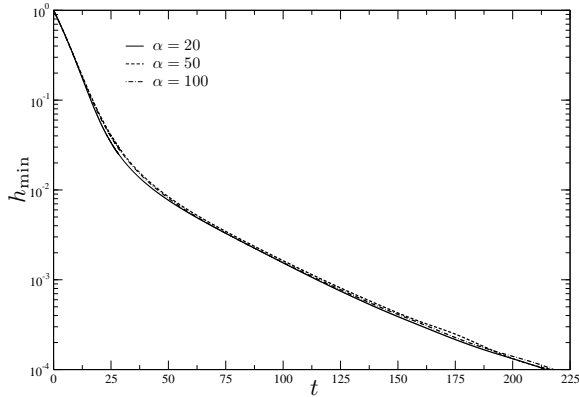


Figure 5: Minimum of h in the liquid film as a function of time for $\alpha = 20, 50,$ and 100 .

The density is equal to 2350 kg/m^3 , the dynamic viscosity is equal to $50 \text{ Pa}\cdot\text{s}$, corresponding to molten glass at $1240 \text{ }^\circ\text{C}$. The surface tension, γ_0 is equal to 0.32 N/m using the correlation factors given by Rubenstein (1964). The length and the initial thickness of the liquid film are respectively $L = 3 \cdot 10^{-2} \text{ m}$ and $H_0 = 10^{-3} \text{ m}$. With these characteristic values, the Bond number is equal to $1.94 \cdot 10^3$ and the Reynolds number to $5.85 \cdot 10^{-1}$. In this subsection, the surface tension gradient is assumed equal to zero, i.e. $\text{Ma} = 0$.

The boundary conditions on the bottom used in the numerical method depend on the arbitrary value, α . This subsection discuss the influence of α in the behavior of the film thickness in space and time.

Figure 5 represents the minimum of h in the liquid film as a function of time for three value of α . The graph is represented in semi-log scales. The film thickness decreases rapidly in the first times and after the thinning rate is slower when t is larger than 50. The first decrease is mainly due to the initial condition assuming an uniform thickness. Close to the top of the liquid film a meniscus appears as soon as the drainage starts as it is shown in the previous subsection. The second part of the thinning process is a properly speaking due to the drainage. As expected, the film thickness decreases exponentially with the time due to the pure extensional flow in the film.

The effect of the boundary conditions at the bottom gives a small effect on the drainage of the liquid film. The thinning rates for the three values of α are similar. The thinning rates are quasi-identical for the three values of α .

In Figure 6, the film thickness is plotted versus x for the three values of α and five times. Close to the top, the profiles of h are similar whatever the value of α . The main difference appear close to the bottom of the liquid film and are directly due to α . The spread of the liquid

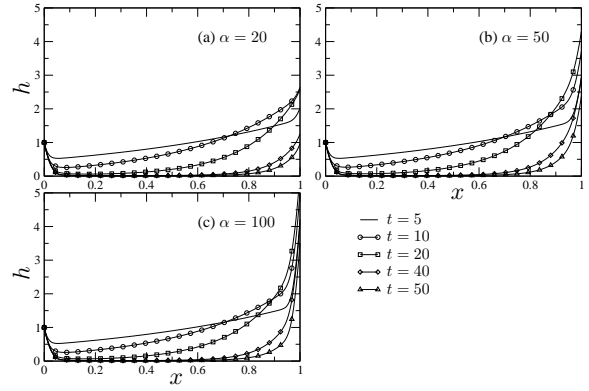


Figure 6: Film thickness, h , as a function of x for (a) $\alpha = 20,$ (b) $\alpha = 50,$ and (c) $\alpha = 100$ and for $t = 5, 10, 20, 40$ and 50 .

film increases obviously with α . Nevertheless, the difference between the results obtained with $\alpha = 50$ and 100 are not very large.

Figure 7 gives the velocity profile for the three values of α and the same times used in Figure 6. The main advantage of the boundary conditions (64) and (65) is that the velocity is not specified at the bottom but is a solution of the problem. Since the spread of the liquid film increases with α , the velocity at the bottom is over estimated when α is small as a result of the mass conservation. The result is true for $\alpha = 20$. In contrary, the velocity profiles are quasi-similar for $\alpha = 50$ and 100 . The velocity calculated at the bottom are very similar for these two values of α . Nevertheless, when $\alpha = 100$, a shoulder is observed for $t = 50$.

Finally, remark that even if it is not easy to see in Figure 7, the velocity is lightly negative close to the top of the liquid film as a consequence of the suction of the boundary where the liquid film is larger that the film thickness far away the top boundary.

The results show that the boundary conditions given by Eqs. (64) and (65) are relevant to describe numerically the matching with the liquid pool. We do not need a boundary condition for the velocity on the bottom. The velocity is a solution of the boundary conditions used to match with the static meniscus. In the following, numerical computations are done with $\alpha = 100$.

5.3. Effect of the surface tension gradient

The surface tension and its gradient are determined for the same glass used in the previous subsection. The quantity $\delta\gamma$ given by (9) is equal to $3.4 \cdot 10^{-2} \text{ N/m}$ using the coefficient factors given by Rubenstein (1964). The conditions used in the numerical simulations are

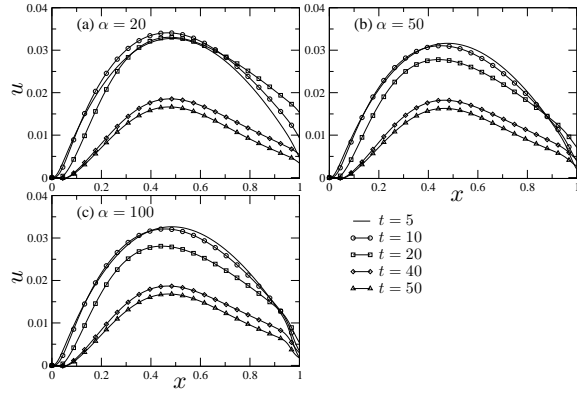


Figure 7: Film velocity, u , as a function of x for (a) $\alpha = 20$, (b) $\alpha = 50$, and (c) $\alpha = 100$ and for $t = 5, 10, 20, 40$ and 50 .

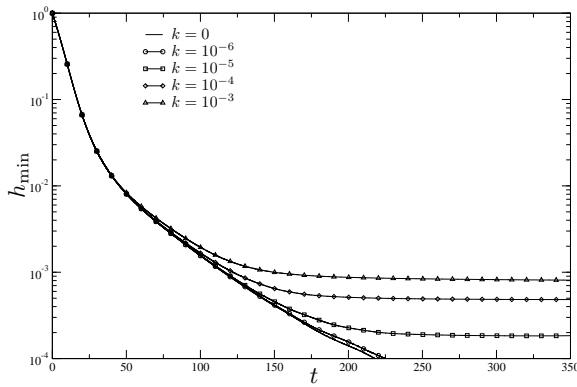


Figure 8: Minimum of h in the liquid film as a function of time for $k = 0, 10^{-6}, 10^{-5}, 10^{-4}$ and 10^{-3} .

identical to those used in the previous subsection. The Marangoni number is equal to $1.64 \cdot 10^{-3}$.

First, the effect of k is addressed by plotting the minimum of h as a function of time. The numerical computations are operated until the minimum of h reaches the dimensionless value equal to 10^{-4} corresponding to a thickness around 100 nm when H_0 is equal to 1 mm. Figure 8 shows the behavior of the minimum of the film thickness versus time for five values of k . The case of $k = 0$ means that the surface tension gradient are equal to zero. When $k = 10^{-6}$, the surface tension gradient is too small to see an effect on the drainage for a typical thickness of 10^{-4} . In contrary, when k is larger than 10^{-6} , the behavior of film thickness changes strongly when h is sufficiently small. Indeed, a steady-state regime is observed after drainage. The asymptotic film thickness increases with k due to the surface tension gradient appears sooner when k is larger.

Film thickness profiles for $t = 200$ for the five values

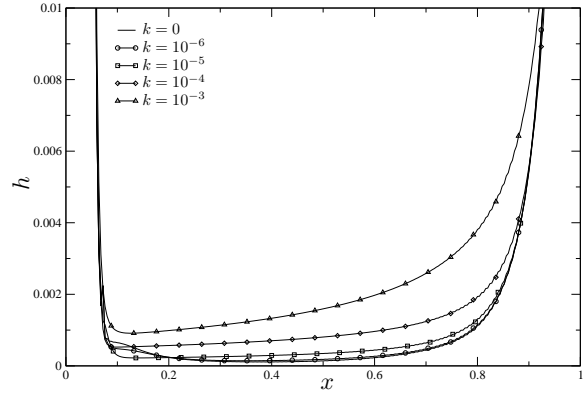


Figure 9: Film thickness, h , as a function of x for $k = 0, 10^{-6}, 10^{-5}, 10^{-4}$ and 10^{-3} when $t = 200$.

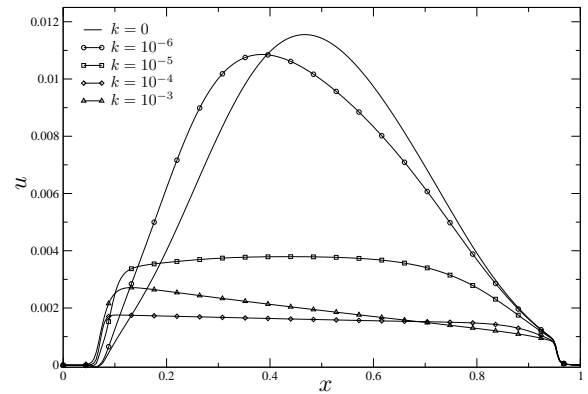


Figure 10: Film velocity, u , as a function of x for $k = 0, 10^{-6}, 10^{-5}, 10^{-4}$ and 10^{-3} when $t = 200$.

of k are plotted in Figure 9. The film profile does not change for k equal to 0 and 10^{-6} . For $k = 10^{-5}$, the film thickness is slightly thicker in the middle of the liquid film. Close to the top and the bottom, the film thickness is very similar to the profiles obtained with $k = 0$ and $k = 10^{-6}$.

The main differences are significant on the film velocity as it can be seen in Figure 10 where u is plotted versus x for the five values of k . The typical velocity decreases by a factor 3 when k increases from 0 to 10^{-5} . Remark, all profiles are close together near the bottom. The velocity profile observed for $k = 10^{-4}$ does not change a lot apart from the top and the bottom with a value smaller than one obtained for $k = 10^{-3}$. For this last value of k , the velocity decreases from the top to the bottom due to the largest heterogeneities in the film thickness observed in Figure 9.

With $k = 10^{-5}$ corresponding to a dimension value around 10^{-8} m, the film thickness reaches an asymptotic value equal to $1.8 \cdot 10^{-4}$ (around 180 nm in dimension unit) meaning that the surface tension varies in the

range of [1; 1.005]. So, an increase of 0.5 % is enough to stabilize the film thickness. Moreover, the equilibrium thickness found with this value are close to the experimental value given by Laimböck (1998) who found a value equal to 200 nm. Kappel et al. (1987) pointed out a value smaller (100 nm) but they did not measured the film thickness carefully. When k is larger than 10^{-5} , the equilibrium thicknesses seems too large comparable to the previous results given in Laimböck (1998) and Kappel et al. (1987).

These experiments done in Laimböck (1998) and Kappel et al. (1987) were achieved in laboratory furnaces where the thermal homogeneities must be controlled. Indeed, a thermal gradient can also changes the surface tension. Scholze (1990) indicates a coefficient a surface tension thermal gradient equal around $4 \cdot 10^{-5}$ N/(mK) meaning that to have an increase of 0.5 % of the surface tension, the difference of the temperature must be equal to 40 K. This thermal difference must be appeared over the liquid length, typically few centimeters, which is too large with laboratory furnaces where the thermal heterogeneities are usually smaller than 10 K in the area of working space. So, the stabilization of the liquid film must be mainly due to the chemical effect.

6. Conclusion

In this work, a lubrication model is introduced to study the drainage of vertical liquid films taking into account the surface tension gradient. The lubrication model is numerically solved with a finite difference method with an implicit time solver.

The numerical procedure is tested on vertical film with a thickness and a velocity specified at the two extremities. The numerical results are compared with prior results obtained analytically. Afterwards, the numerical procedure is applied to study the drainage of molten glass with a composition close to a window glass. We show that the chemical effect leading to the surface tension gradient can stabilize the liquid film at a thickness in agreement with observed results achieved by Laimböck (1998).

These results point out that even if a molten glass is usually considered with interface without “surfactant agents”, the evaporation of oxides like Na_2O toward interface can lead to a stabilization of gravitational drainage of vertical film. This effect is very important for applications because it can explain why a significant foam layer appears in glass furnaces.

Even if the segregation of various oxides leading to a surface tension gradient of molten glass can be formulated in a theoretical model as it is done in this work, the driven forces giving this segregation is not explained here and must be investigated in the future.

A. Derivation of the boundary condition at the bottom of the liquid film

The equation of the static meniscus is given by Eq. (23). By multiplying Eq. (23) by κ and integrating over x , the following relationship is obtained

$$\kappa^2 = -\frac{h_{,x}}{l_c^2 \sqrt{1 + h_{,x}^2/4}} + \frac{A}{l_c^2}, \quad (79)$$

where A is an integration constant.

For a film falling in a large pool, the free surface can be considered as flat meaning that $h_{,x}$ goes to infinity when $x \rightarrow L$. Since the curvature must be equal to zero, A must be equal to 2. Finally, under dimensionless form, if we specify, the first derivative of h at the bottom of the film, the second derivative is given by Eq. (65).

References

- R. G. C. Beerkens. Modeling the kinetics of volatilization from glass melts. *J. Am. Ceram. Soc.*, 84:1952–1960, 2001.
- R. J. Braun, S. A. Snow, and U. C. Pernisz. Gravitational drainage of a tangentially immobile thick film. *J. Colloid Interface Sci.*, 219:225–240, 1999.
- R. J. Braun, S. A. Snow, and S. Naire. Models for gravitationally-driven free film drainage. *J. Eng. Math.*, 43:281–314, 2002.
- L. Collatz. *The numerical treatment of differential equations*. Springer-Verlag, Berlin, 1960.
- P.-G. de Gennes. “Young” soap films. *Langmuir*, 17: 2416–2419, 2001.
- B. Déminovith and I. Maron. *Eléments de calcul numérique*. Editions Mir, Moscou, 1979.
- C. A. J. Fletcher. *Computational Techniques for Fluid Dynamics. Volume I: Fundamental and General Techniques*. Springer-Verlag, Berlin, 1991.
- P. D. Howell. Models for thin viscous sheets. *Eur. J. Appl. Math.*, 7:321–346, 1996.
- J. Kappel, R. Conradt, and H. Scholze. Foaming behaviour on glass melts. *Glastech. Ber.*, 60:189–201, 1987.
- D.-S. Kim and P. Hrma. Foaming in glass melts produced by sodium sulfate decomposition under ramp heating conditions. *J. Am. Ceram. Soc.*, 75:2959–2563, 1992.

P. Laimböck. *Foaming of glass melts*. PhD thesis, Technische Universiteit Eindhoven, 1998.

S. Naire, R. J. Braun, and S. A. Snow. An insoluble surfactant model for a vertical draining free film. *J. Colloid Interface Sci.*, 230:91–106, 2000.

F. Pigeonneau, H. Kočárková, and F. Rouyer. Stability of vertical films of molten glass due to evaporation. *Colloids Surf., A*, 408:8–16, 2012.

L. Pilon. *Interfacial and transport phenomena in enclosed cell foam*. PhD thesis, Purdue University, 2002.

W. H. Press, B. P. Flannery, S. A. Teukolsky, and W. T. Vetterling. *Numerical recipes in FORTRAN. The art of scientific computing*. Cambridge University Press, Cambridge, 1992.

C. Rubenstein. Factors for the calculation of the surface tension of glasses at 1200 C. *Glass Technol.*, 5:36–40, 1964.

E. Ruckenstein and R. K. Jain. Spontaneous rupture of thin liquid films. *J. Chem. Soc., Faraday Trans. 2*, 70:132–147, 1974.

K. J. Ruschak. Flow of a falling film into a pool. *AIChE J.*, 24:705–709, 1978.

D. M. Sanders and W. K. Haller. Effect of water vapor on sodium vaporization from two silica-based glasses. *J. Am. Ceram. Soc.*, 60:138–141, 1977.

B. Scheid, E. A. van Nierop, and H. A. Stone. Thermocapillary-assisted pulling of thin films: Application to molten metals. *Appl. Phys. Lett.*, 97:171906–1–3, 2010.

H. Scholze. *Glass. Nature, Structures and Properties*. Springer-Verlag, Berlin, 1990.

L. W. Schwartz and R. V. Roy. Modeling draining flow in mobile and immobile soap films. *J. Colloid Interface Sci.*, 218:309–323, 1999.

J. E. Shelby. *Introduction to Glass Science and Technology*. The Royal Society of Chemistry, Cambridge, 1997.